Extreme ultra-violet laser ablation of solid targets

G J Tallents[a***], S A Wilson[a*], J Lolley[a], V Aslanyan[a+], A West[a++], A K Rossall[a**], E Solis-Meza[a], E Wagenaars[a], C S Menoni[b] and J J Rocca[b]

[a]York Plasma Institute, Department of Physics, University of York, York YO10 5DD, U.K.
[b]Center for Extreme Ultraviolet Science and Technology and Department of Electrical and Computer Engineering, Colorado State University, Fort Collins, Colorado 80523, U.S.A.
[*]Now at XUV Lasers, PO Box 273251, Fort Collins CO 80527-3251, U.S.A.
[+]Now at MIT PSFC, 175 Albany Street, Cambridge, Massachusetts 02139, U.S.A.
[++]Now at School of Electrical and Electronic Engineering, University of Manchester, Manchester, U.K.
[**]Now at School of Engineering and Computing, University of Huddersfield, Huddersfield, HD1 3DH, U.K.

ABSTRACT

A capillary laser with output in the extreme ultra-violet at wavelength 46.9 nm is used to ablate solid targets of parylene-N (CH), PMMA, aluminum and gold. We summarize results obtained using different focusing optics: a Fresnel zone plate, an off-axis spherical multi-layer mirror and on-axis multi-layer and gold mirrors. The Fresnel zone plate has a small aperture and focuses a small fraction of the laser energy to a small diameter (< 1 μm) with peak intensities 6 x 10^9Wcm^{-2}. The off-axis spherical multi-layer mirror allows for a measurement of the transmission of the laser through thin targets, but the off-axis geometry produced an aberrated focus. The on-axis multi-layer mirror allows focusing to intensities of approximately 5 x 10^{10} Wcm^{-2} with a cylindrically symmetric focus.

Keywords: extreme ultra-violet, laser, capillary, ablation

1. INTRODUCTION

Laser output in the extreme ultra-violet/soft x-ray regime has been created (i) in free electron lasers where electron beams oscillating in alternating magnetic fields create laser output and (ii) by using atomic processes in hot plasmas. The generation of short wavelength laser light in hot plasmas alongside applications of short wavelength laser light, have been the themes of this SPIE series of conferences [1]. Saturation of laser output occurs when stimulated emission reduces the small signal gain coefficient. Saturation is regarded as a key milestone in short wavelength laser development as the laser output is typically a factor 10^4 - 10^6 larger than can occur without stimulated emission and the laser output energy is extracted with optimum efficiency if saturation occurs.

Work using hot plasma as the medium for lasing output at short wavelength has resulted in saturated amplified spontaneous emission at wavelengths as short as 5.86 nm with the plasma created using a 6-beam high power optical laser [2]. By optimizing the angle of incidence of the optical laser beams creating the plasma medium, saturated tabletop lasers over the wavelength range 16.5 – 13.9 nm were produced with only 1 J per pulse of the optical laser [3]. The work on soft x-ray lasers pumped by optical lasers has created useful short wavelength lasers for applications and led to a greater understanding of laser-plasmas and the atomic physics of hot plasmas which has relevance to much wider fields of study [4].

As well as using plasmas created by optical lasers to produce the required plasma medium [5], a laser operating at wavelength 46.9 nm pumped by electrical discharge in an argon plasma confined to a capillary has been developed [6]. This capillary laser operates at wavelength 46.9 nm with output over typically 1 – 1.5 ns with achieved energy per pulse up to 1 mJ. As the capillary laser has power supplies and footprint suitable for a small laboratory, potential industrial and laboratory applications are being investigated [7 – 9]. There is also interest in capillary discharge plasmas for other applications as the plasma formed is uniform along its length for typically 20 cm [10].

***greg.tallents@york.ac.uk

We use here a capillary laser with energy per pulse of 50 μJ. We investigate different focusing arrangements to ablate solid targets. The direct ablation of solid targets with short wavelength laser light may have applications in the manufacture of micro electro-mechanical systems (MEMS) [13] and the plasmas produced have interesting properties as they are typically of high solid density, but low temperature (< 10 eV). Such plasmas are referred to as 'warm dense matter' and are relevant to the physics of the interiors of large planets and to laser fusion [14]. We report results here on the ablation craters formed by the focused extreme ultra-violet (EUV) laser light at 46.9 nm.

2. THE THEORY OF EUV ABLATION

The modeling and simulation of the interaction of 46.9 nm radiation with solid targets has been investigated in previous publications by the authors. The two-dimensional fluid code POLLUX was modified to include laser absorption by direct photo-ionization using a super-configuration model to describe the ionization dependent electron distributions [11]. Direct photo-ionization occurs in atoms with ionization energy less than the capillary laser photon energy (26.4 eV) so that solid target material is initially opaque to the laser radiation and bleaches to transparency as the material is ionized. For target material with a short attenuation length to 46.9 nm radiation (at room temperature), this leads to a traveling ionization wave of ablation as subsequent short distances in the target bleach to transparency during the laser pulse. Once ionization has occurred, inverse bremsstrahlung also occurs in the ablating plasma [12]. As the plasma density is high (close to solid) and the temperatures produced in the expanding plasma are low (< 10eV), free electron degeneracy effects in the plasma can modify the absorption coefficients for photo-ionization and inverse bremsstrahlung [12].

If the attenuation length to 46.9 nm radiation (at room temperature) is long, ablation occurs over the attenuation length to a depth determined by some ablation threshold fluence [12]. During the laser pulse duration (1.3 ns in our case), there is insufficient bleaching for the ionization wave ablation to commence. For example, gold with an attenuation length at 46.9 nm of 6×10^{-3} μm exhibits ionization wave ablation, while aluminum with an attenuation length at 46.9 nm of 0.41 μm ablates to a depth determined by an ablation threshold (for aluminum 1.2 Jcm^{-2}).

3. ABLATION WITH A FRESNEL LENS

A capillary discharge laser was focused using a Fresnel zone plate lens onto a planar parylene-N target [13]. The Fresnel zone plate only focuses approximately 3% of the laser beam with a numerical aperture of 0.12. Assuming a uniform laser intensity profile across the lens, a focus with the first null of the Airy disk with a diameter of 240nm is possible. However, craters with a full width at half-maximum diameter between 650 and 850nm were ablated by the laser (see e.g. figure 1).

Figure 1(a) shows a post-shot image of an ablated parylene-N target measured using atomic force microscopy (AFM) for a laser fluence of 7.7 J cm^{-2} corresponding to a peak intensity of 6×10^{9} Wcm^{-2}. The corresponding line-out through the central ablated region is shown in figure 1(b) along with a comparison to two different ablation profile simulated with the POLLUX code. One of the assumed profiles considers a Gaussian profile, while the second assumes a double Gaussian profile to approximate an Airy pattern with 92% of the energy in the central lobe and 8% of the energy in a side lobe. The depth of ablation in the simulation shown in figure 1 is taken at time 1.3 ns at the end of the laser pulse where the ion temperature equals the melting point for parylene-N (0.06 eV). This experiment has been reported in greater detail by Rossall et al [13].

4. ABLATION WITH AN OFF-AXIS SPHERICAL MIRROR

In order to ablate a target at moderate to high irradiance and simultaneously measure the EUV laser transmission through the target, a capillary laser beam was focused by a single spherical scandium-silicon multilayer mirror (M1) with a focal length of 50 mm, tilt of 4.7° and approximate numerical aperture of 0.05 (see figure 2). The use of a multilayer mirror enabled the full spatial output of the capillary laser to be focused. A second identical mirror (M2) recollimated the beam, so that the transmission through the approximately 1 μm thick parylene-N (CH) target was measured by a back-thinned CCD camera. This experiment and the analysis of the transmission have been reported in greater detail by Aslanyan et al [15].

The intensity profiles at the targets were modeled by solving the Fresnel diffraction integral and compared to post-shot microscope images of the damage to the parylene targets (see figure 2). The incident EUV laser beam profile was

measured with the CCD camera and the reflection properties of the multilayer mirrors were simulated by the IMD code [16] for a range of angles of incidence. Allowing for the tilted spherical surface geometry of the mirror, the diffraction integral on a series of planes at various distances close to the focal length of the mirror were modeled by solving the appropriate Fresnel diffraction integral. Contours representing the threshold intensity (10^9 Wcm^{-2}) for ablation of the targets are superimposed on figure 2. The mirror-target distance is estimated to be approximately 50 μm from the optimum focus so the intensity on target is dominated by aberrations largely arising due to the tilting of the focusing mirror.

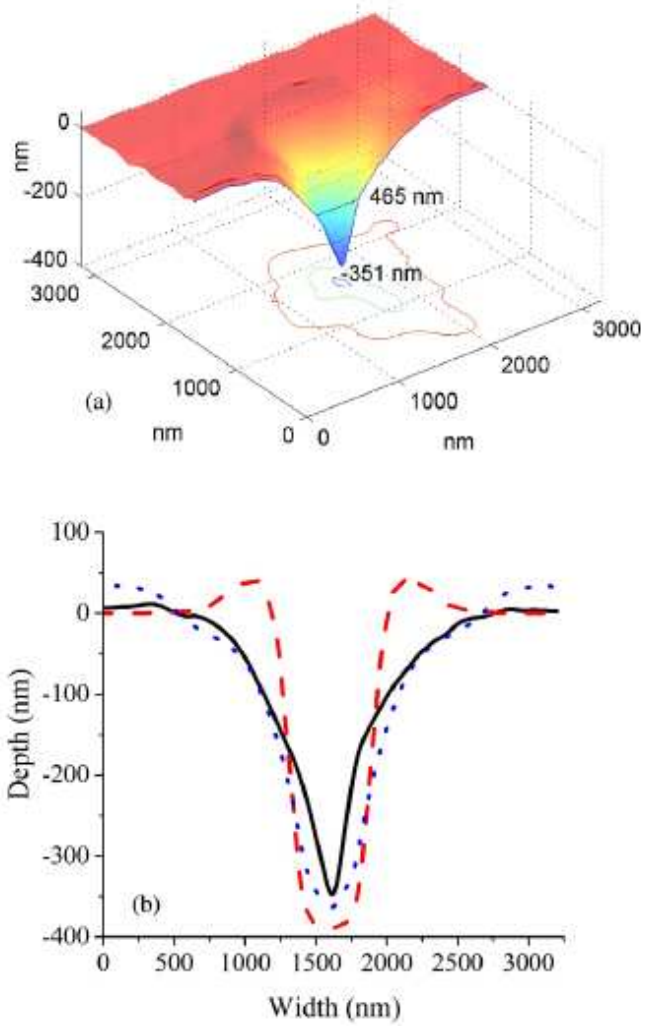

Figure 1. An experimentally measured ablation profile in PMMA obtained using a Fresnel lens with fluence on target of 7.5 J cm^{-2} giving a peak intensity of 6 x 10^9 Wcm^{-2} (upper plot). A cross-section of the ablated depth is shown as a solid curve (lower plot). Simulated ablation profiles are also shown (lower plot) assuming a Gaussian beam profile (red broken curve) and a double Gaussian with 92% of beam energy in a central Gaussian and 8% in a wider Gaussian (blue dotted curve).

The target ablation and the expansion of plasma created by absorption of the focused EUV laser beam was simulated using the 2-dimensional radiation-hydrodynamic code POLLUX [13]. The POLLUX code incorporates a comprehensive equation of state model with appropriate phase transitions. The distribution of ion charge is modeled assuming local thermodynamic equilibrium (LTE) allowing for ionization potential depression. The opacity at wavelength 46.9 nm due to photoionization and inverse bremsstrahlung is evaluated. Ablation of solid-density material by EUV radiation creates a low-density plume of plasma expanding in the direction of the laser and (more slowly) laterally. For intensities

considered in this paper, the plasma density drops approximately exponentially along the laser axis. The peak electron temperature $k_B T_e \simeq 5$ eV occurs close to the ablation front. At times before ablation through the target, we find that the EUV transmission is zero, only becoming significant where the target is fully ablated and the plasma is ionized to C^{2+} (where the ionization potential of 47.9 eV is above the photon energy of 26.4 eV). Transmission of laser light through the target is thus a diagnostic of ablation through the target thickness of 1028 nm. Comparisons of calculated intensity profiles transmitted through the target show the same diffraction pattern as the intensity profiles recorded by the CCD camera (e.g. figure 3).

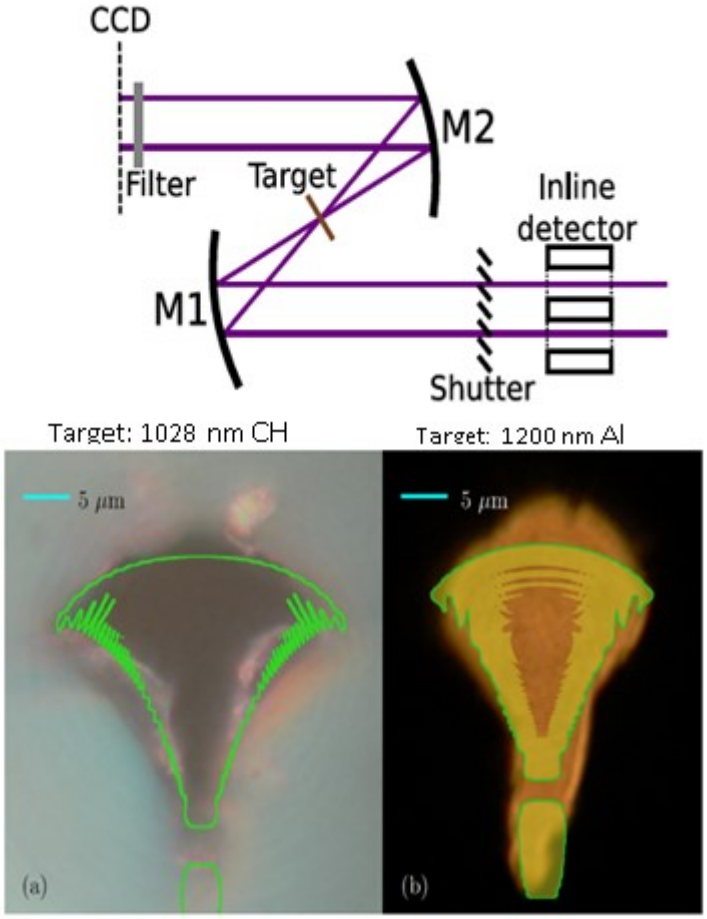

Figure 2. A schematic of the focus and collection of transmitted laser light with a spherical mirrors tilted at 4.7° (upper schematic). Microscope images of CH and Al targets irradiated by the capillary laser are shown (lower images as labelled) with a superimposed calculation of an irradiance contour in green corresponding to 10^9 Wcm^{-2}.

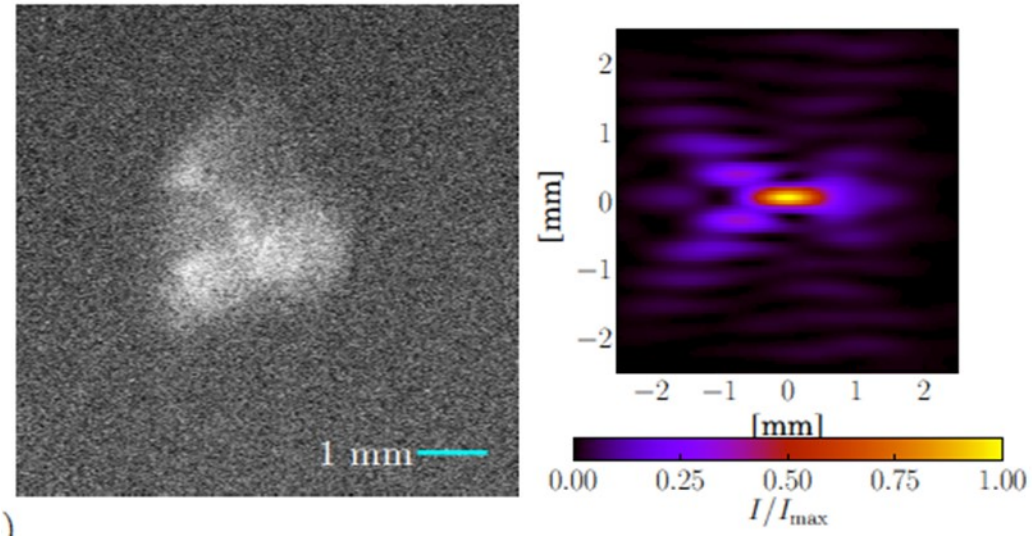

)

Figure 3. The laser light transmitted through a 1028 nm thick CH target by a focused capillary laser as measured using an identical collecting mirror to the focusing mirror (left side). The calculated transmission of laser light (right side) is calculated assuming a transmitted intensity profile such that the transmission is only non-zero where ablation through the target has occurred. The distance scale of 1 mm at the focal length of 50 mm corresponds to diffraction of 20 milliradians from the ablated target.

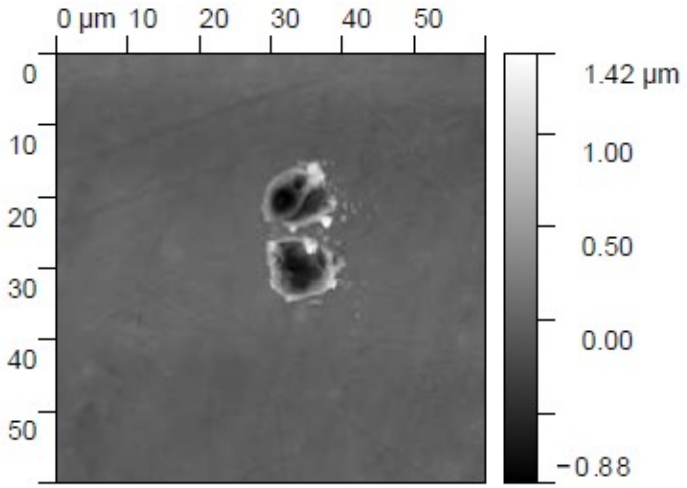

Figure 4. An atomic force microscope image of ablation craters in an aluminium target which is 100 µm out of focus. The double spot arises due to diffraction of the incoming laser beam around the 1 mm wide target before light reaches the focusing lens.

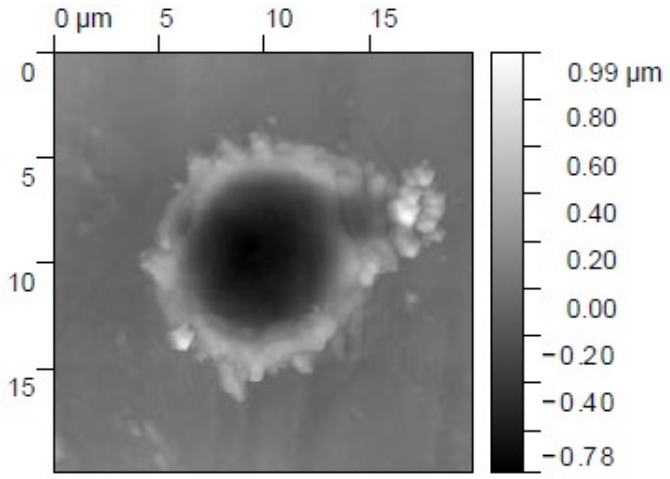

Figure 5. An atomic force microscope image of the ablation crater produced in a gold target from a single capillary laser shot close to best focus.

5. ABLATION WITH AN IN-LINE SPHERICAL MIRROR

Focusing the laser without a mirror tilt minimises the aberrations discussed in section 3, but does not enable a measure of laser transmission through the target. The spherical mirrors positioned normal to the capillary laser output at wavelength λ = 46.9 nm were used to focus the laser beam onto narrow strip targets of 1 mm width. As in section 3, one mirror had a scandium-silicon multilayer coating (giving a reflectivity of approximately 0.45), while another was a solid gold mirrors (with a reflectivity of approximately 0.08). The 1 mm wide targets intercepted the incoming laser beam and exhibit diffraction effects (see figure 4). We expect the d_t = 1 mm targets to produce an angular change θ of the laser components either side given by $\theta \cong \lambda / d_t$. Out of focus when the laser light is focused back onto the target in the near-field, two beamlets are focused with a separation given by

$$\Delta l = 4 f \theta \tag{1}$$

where f = 50 mm is the focal length of the spherical mirror. The experimental value of Δl = 9.4 µm measured from figure 4 agrees with the value determined using equation 1. Scanning the mirror-target distance with many shots enabled the best focus distance to be determined. At the optimum focus, a smaller single focal spot is obtained (see figure 5). The production of two ablation craters out of focus due to diffraction around the target and a single crater in focus, is evidence that the laser output has coherence over 1 mm at the target distance of 1.4 m from the laser. This implies coherence over angles approaching at least 1 mrad. As the full spatial profile of the laser was focused with the in-line multilayer mirror, the focused laser fluence for figure 6 is approximately 50 Jcm^{-2} corresponding to a peak laser intensity of 5 x 10^{10} Wcm^{-2}.

6. CONCLUSION

A capillary laser with output in the extreme ultra-violet at wavelength 46.9 nm has been used to ablate solid targets of parylene-N (CH), aluminum and gold. Results obtained using different focusing optics have been presented: a Fresnel zone plate, an off-axis spherical multi-layer mirror and on-axis multi-layer and gold mirrors. The Fresnel zone plate has a small aperture and focuses a small fraction of the laser energy to a small diameter (< 1 µm) with peak intensities 6 x 10^9 Wcm^{-2}. The off-axis spherical multi-layer mirror allows for a measurement of the transmission of the laser through thin targets, but the off-axis geometry produced an aberrated focus. The on-axis multi-layer mirror allows focusing to intensities of approximately 5 x 10^{10} Wcm^{-2} with a cylindrically symmetric focus.

ACKNOWLEDGEMENTS

The authors acknowledge funding from AWE Plc., the Engineering and Physical Science Research Council (Grant nos. EP/J019402/1 and EP/K504178/1) and Heriot-Watt University 'Centre for Innovative Manufacturing in Laser-based production processes' (grant no. EP/K030884/1).

REFERENCES

[1] Tallents, G. J. et al, "Improving the efficiency of x-ray lasers," Proc. SPIE **2520**, 34-44 (1995). DOI: 10.1117/12.221650

[2] Smith, R., Tallents, G. J., Zhang, J., Eker, G., McCabe, S., Pert, G. J. and Wolfrum E., "Saturation behavior of two x-ray lasing transitions in Ni-like Dy," Phys. Rev. A**1**, R47-R50 (1999).

[3] Wang, Y., Larotonda, M. A., Luther, B. M., Alessi, D., Berrill, M., Shlyaptsev, V. N. and Rocca, J. J., "Demonstration of high-repetition-rate tabletop soft-x-ray lasers with saturated output at wavelengths down to 13.9 nm and gain down to 10.9 nm," Phys. Rev. A**72**, 053807 (2005).

[4] Tallents, G. J., [An introduction to the atomic and radiation physics of plasmas], Cambridge University Press, Cambridge, (2018).

[5] Tallents, G. J., "The physics of soft-ray lasers pumped by electron collisions in laser plasmas," J. Phys. D., **36**, R259-R276 (2003).

[6] Benware, B. R., Macchietto, C. D., Moreno, C. H. and Rocca, J. J., "Demonstration of a high average power tabletop soft x-ray laser," Phys. Rev. Lett., **81**, 5804-5807 (1998).

[7] Brewer, C. A. et al, "Single-shot extreme ultraviolet laser imaging of nanostructures with wavelength resolution," Optics Lett. **33**, 518-520 (2008).

[8] Kuznetsov, I, Filevich, J. Dong, F., Woolston, M, Chao, W., Anderson, E. H. Anderson, Bernstein, E. R., Crick, D., Rocca, J. J. and Menoni, C. S., "Three-dimensional nanoscale molecular imaging by extreme ultraviolet laser ablation mass spectrometry," Nat. Commun. 6:6944 (2015).

[9] Straus, J., Kolacek, K., Schmidt, J., Frolov, O., Vilemova, M., Matejicek, J., Jager, A., Juha, L., Toufarova, M., Choukourov, A. and Kasuya, K., "Response of fusion plasma-facing materials to nanosecond pulses of extreme ultraviolet radiation," Laser Part. Beams 1-15 (2018).

[10] Page, T., Wilson, S. A., Branson, J., Wagenaars, E. and Tallents, G. J., "Plasma temperature measurement using black-body radiation from spectra lines emitted by a capillary discharge," J. Quant. Spect. Rad. Trans. **220**, 1-4 (2018).

[11] Rossall, A. K. and Tallents, G. J., "Generation of warm dense matter using an argon based capillary discharge laser," High Energy Density Phys., **15**, 67-70 (2015).

[12] Lolley, J. A., Wilson, S. A. and Tallents, G. J., "Modeling extreme ultraviolet ablation interactions," Proc. SPIE **11035**, R1-R8 (2019).

[13] Rossall, A. K., Aslanyan, V., Tallents, G. J., Kuznetsov, I., Rocca, J. J. and Menoni, S., "Ablation of submicrometer holes using an extreme ultraviolet laser," Phys. Rev. Appl. **3**, 064013 (2015).

[14] Tallents, G. J., Wilson, S., West, A., Aslanyan, V., Lolley, J. and Rossall, A. K., "The creation of radiation dominated plasmas using laboratory extreme ultra-violet lasers," High Energy Density Phys., **23**, 129-132 (2017).

[15] Aslanyan, V., Kuznetsov, I, Bravo, H., Woolston, M. R., Rossall, A. K., Menoni, C. S., Rocca, J. J. and Tallents, G. J., "Ablation and transmission of thin solid targets irradiated by intense extreme ultraviolet laser radiation," APL Photonics **1**, 066101 (2016).

[16] Windt, D. L., Comput. Phys. **12**, 360 (1998).